Evaluation of Magnetic Fields inside High Voltage Substations with Different Configurations

Samy M. Ghania
University of Jeddah, Jeddah, Saudi Arabia
sghania@uj.edu.sa (corresponding author)

Received: 22 October 2023 | Revised: 12 November 2023 | Accepted: 15 November2023

 DOI: https://doi.org/10.48084/etasr.6554

ABSTRACT

The exposure risk of magnetic fields produced inside high-voltage substations is still a challenging issue for both utility design engineers and biomedical researchers. There are two different types of exposure, the first type is the public type which comes from any temporary human presence near any electrical utility installation while the second type is the residential which comes from any type of residency or semi-permanent presence for more than 8 hours (working shifts) nearby any electrical utility installation. This classification is mainly dependent upon the levels and durations of exposure. This paper presents the full simulation for two typical high voltage substations of 500/220 kV and 220/66 kV with different bus bar configurations for calculating the magnetic field distributions. The effects of different bus bar configurations on the magnetic field levels are presented. The simulated results are compared with the measured values to validate the simulation accuracy.

Keywords-high voltage substations; magnetic fields; different configurations

I. INTRODUCTION

Power frequency (50/60 Hz) magnetic fields, especially those produced nearby power lines and inside electrical installations are a major concern of public and utility engineers, due to the probable interactions they have with living organisms [1, 2]. The magnetic fields are produced in many different environments where current-carrying conductors exist, such as in the case of electric power transmission and distribution overhead lines, cables, and substations. Many studies have examined the magnetic fields produced by the electric power transmission lines and electric power substations [3-9]. The potential hazards and biological effects of the magnetic fields on the human health have been addressed in multiple researches [10, 11]. Several countries are following the guidelines given by the International Commission on Non-Ionizing Radiation Protection which sets a value of 100 μT (1000 mG) for 50 Hz magnetic field exposure for the general public and 500 μT (5000 mG) for occupational exposure therefore, utilities are aware that the public's concerns about this issue are widespread and sincere [12]. The SUBCALC program is used to model the magnetic fields in a 230 kV substation in [13]. SUBCALC magnetic field modeling program is developed by EPRI environment division and runs under Microsoft Windows. This program models the power frequency magnetic fields from a user specified array of transmission, primary distribution lines, and substation conductors. The resulting magnetic field has a maximum value of about 30 μT. The calculations within the model are based on the Biot-Savart law governing magnetic fields. This paper presents the results of simulation and measurement of the magnetic fields on a typical 500/220 kV and 220/66 kV substations in Egypt. Measurements of magnetic field are performed using an advanced field meter, HI 3604 ELF survey meter [14, 15].

II. SYSTEM CONFIGURATIONS

Two typical high voltage substations are simulated using the MATLAB – M-Script developer based on Biot-Savart Law in its general form using the (3 D) technique. The actual shape of each section (ingoing, higher voltage bus bar, lower voltage bus bar, and outgoing) of the current-carrying conductor system is divided into a number of connected in series current segments to closely fit the shape of the section and consequently form the whole substation conductor system. Different configurations of the 500/220 kV and 220/66 kV substations are considered (Figures 2-3). The different configurations are:

- Single/double bus bar system with horizontal configurations.
- Double bus bar system with horizontal/vertical configurations.

The different scenarios for the bus bar arrangements and their main dimensions and parameters are shown in Figures 1-4. There are 5 different scenarios for the bus bar arrangement:

- A: Single bus bar with 500/220 kV horizontal arrangements.

- B: Double bus bar with 500/220 kV horizontal arrangements.
- C: Double bus bar with 220/66 kV horizontal arrangements.
- D: Double bus bar with 220/66 kV vertical arrangements.
- E: Double bus bar with all 220/66 kV vertical arrangements.

Figure 2 presents the horizontal and vertical configurations for the 220/66 kV substation. Different bus bar arrangement scenarios were simulated as shown in Figures 3 and 4.

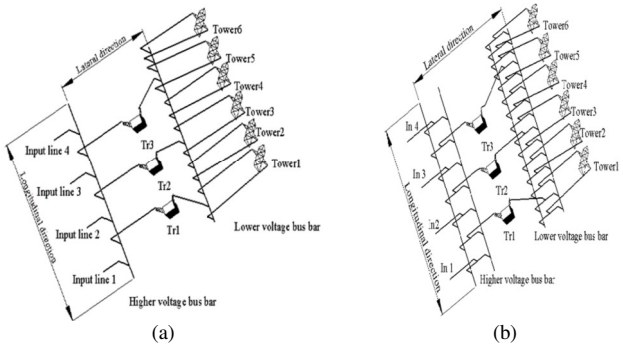

(a) (b)

Fig. 1. Single line diagram for a 500/220 kV substation with single/ double bus bar configuration (Phase A). (a) Single horizontal, (b) double horizontal.

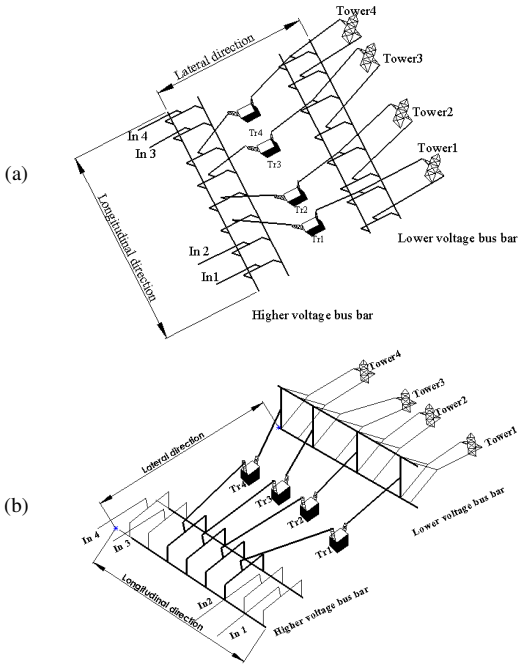

Fig. 2. Single line diagram for the 220/66 kV substation with double bus bar configuration - Phase A (not to scale). (a) Horizontal, (b) vertical.

III. MAGNETIC FIELD CALCULATIONS

Magnetic field calculation techniques can be basically classified into two types. The first type is a two-dimensional (2D) technique in which the power conductors are assumed to have infinitely long segments which are parallel to each other and to the flat ground. The second type is the three-dimensional (3D) technique at which the power conductors are divided into a finite number of segments which are positioned to closely fit the actual shape of the whole conductor system configuration. A 3D technique is used as the base of the present magnetic field calculation [16]. Figure 5 presents an arbitrary carrying-current conductor segment $\vec{a}$ in free space with respect to the reference point O and any random observation point P.

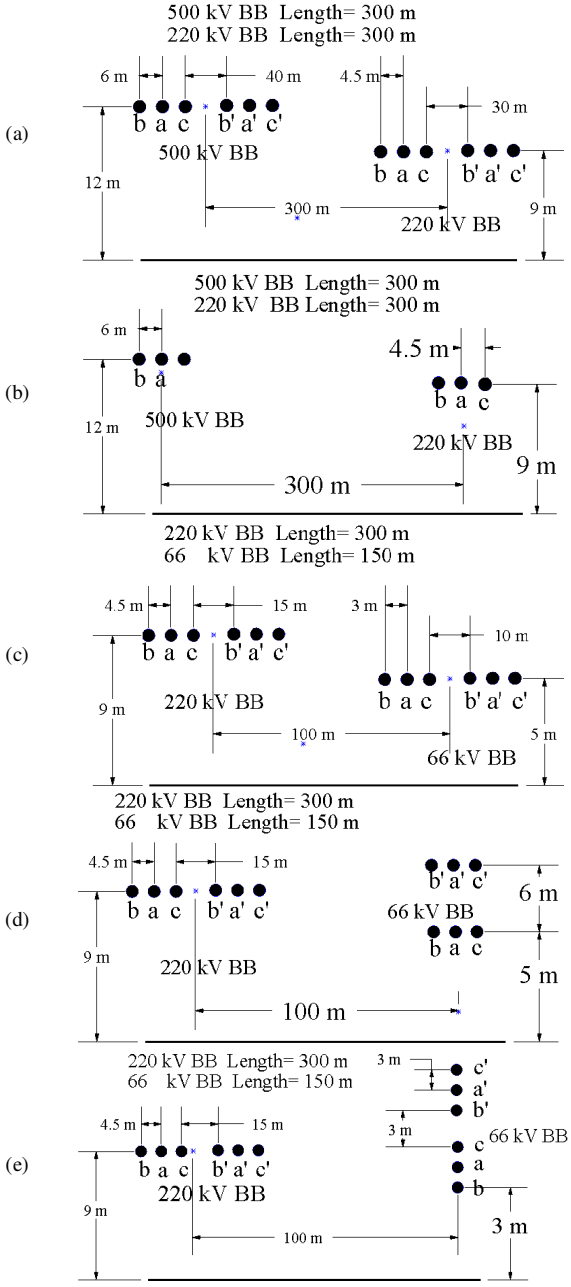

Fig. 3. Different scenarios for bus bar arrangements simulated substations (not to scale). (a) Double bus bar with 500/220 kV horizontal arrangements, (b) single bus bar with 500/220 kV horizontal arrangements, (c) double bus bar with 220/66 kV horizontal arrangements, (d) double bus bar with 220/66 kV vertical arrangements, (e) double bus bars for all 220/66 kV vertical arrangements.

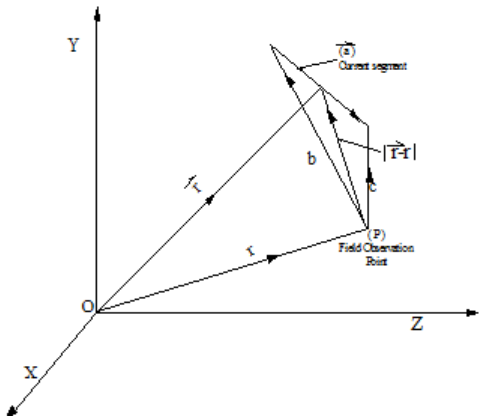

Fig. 4. Presentation of the current segment in free space.

For the current segment $\vec{a}$ carrying current of current density $\vec{J}$, the magnetic field intensity is presented in (1) and with integrating over the volume it can be given as in (2).

$$\left(\vec{H} = \left(\frac{1}{4\pi}\int_v \frac{\vec{J}\times\vec{Z}_{rr}}{|r-\vec{r}|^2}\,dv\right)\right) \quad (1)$$

$$\vec{H} = \left(\frac{\vec{I}}{4\pi}\right)\left(\frac{\vec{c}\times\vec{a}}{|\vec{c}\times\vec{a}|^2}\right)\left(\frac{\vec{a}.\vec{c}}{|\vec{c}|} - \frac{\vec{a}.\vec{b}}{|\vec{b}|}\right) \quad (2)$$

where $\vec{J}$ is the current density in the current segment, $\vec{Z}_{rr}$ is the direction vector between the segment and P, I is the current in the segment, and a, b, and c are vectors.

The magnetic flux density due to the n^{th} current segment is:

$$\vec{B}\,(n) = 0.1\,\vec{I}\left(\frac{\vec{c}\times\vec{a}}{|\vec{c}\times\vec{a}|^2}\right)\left(\frac{\vec{a}.\vec{c}}{|\vec{c}|} - \frac{\vec{a}.\vec{b}}{|\vec{b}|}\right)\mu T \quad (3)$$

Then, for the power line of M conductors, the components of magnetic flux densities and its total magnitude value can be given as:

$$\vec{B}_x = \sum_{m=1}^{M}\vec{B}_x(m)$$
$$\vec{B}_y = \sum_{m=1}^{M}\vec{B}_y(m) \quad (4)$$
$$\vec{B}_z = \sum_{m=1}^{M}\vec{B}_z(m)$$

$$B_{rms} = \sqrt{{B_x}^2 + {B_y}^2 + {B_z}^2} \quad (5)$$

IV. MAGNETIC FIELD CALCULATIONS

A. 500/220 kV Substation

Figure 5 presents the magnetic field distribution over the entire area of the 500/220 kV substation with single bus bar configuration (Scenario A) while all outgoing 220 kV power lines are loaded with 50 MW. The maximum magnetic field value is about 8.3 μT and it is obtained within the area of lower voltage bus bar. Figure 6 presents the magnetic field distribution over the entire area of 500/220 kV substation while the second ingoing power line is switched off. The maximum magnetic field value is still the same while the magnetic field distribution under the area of higher voltage bus bar is affected and its value is increased by about 5%.

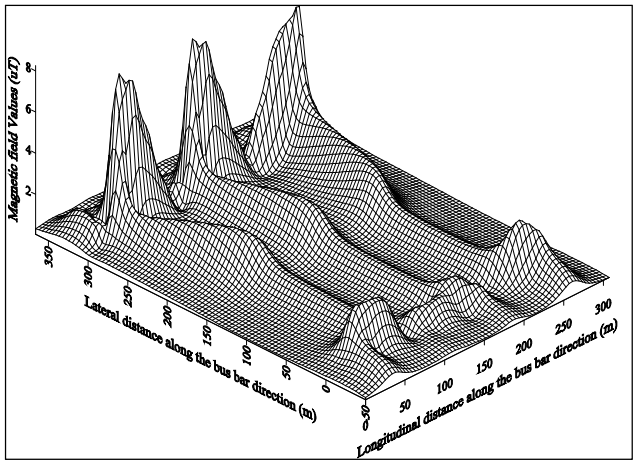

Fig. 5. Magnetic field distribution over the entire area of the simulated 500/220kV substations with single bus bar (Scenario A) configuration and all outgoing lines loaded with 50 MW.

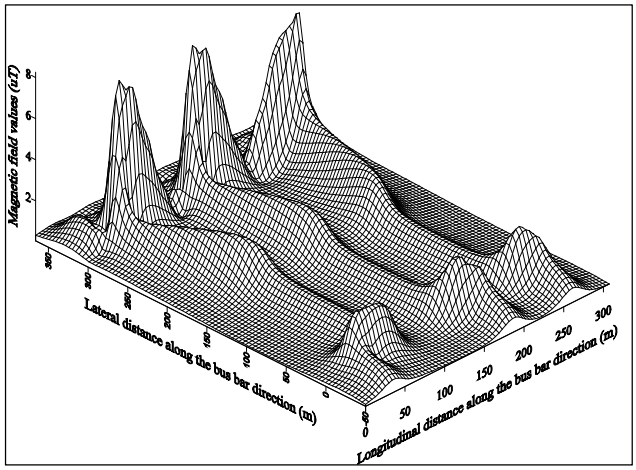

Fig. 6. Magnetic field distribution over the entire area of 500/220 kV substation while the second ingoing power line is switched off.

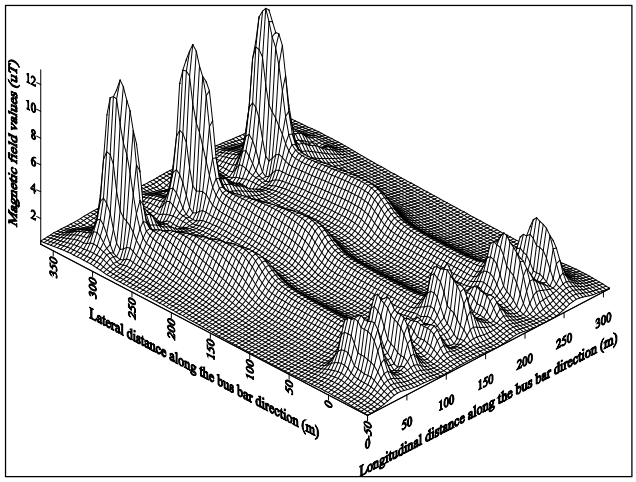

Fig. 7. Magnetic field distribution over the entire area of the simulated 500/220kV substations with double bus bar horizontal configuration (Scenario B).

Figure 7 presents the magnetic field distribution over the entire area of the 500/220 kV substation with double bus bar configuration (scenario B) while all outgoing 220 kV power lines are loaded with 50 MW. The maximum magnetic field value is about 13.2 μT and it is obtained within the area of lower voltage bus bar. Figure 8 presents the magnetic field distribution inside the entire area of 500/220 kV substation with double bus bar configuration, while the second ingoing power line is switched off. The maximum magnetic field value is almost the same while the magnetic field distribution under the area of higher voltage bus bar is affected and its value is increased by about 7%.

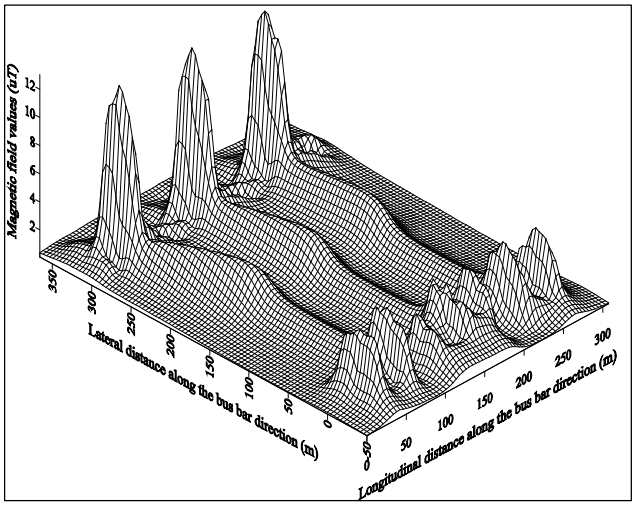

Fig. 8. Magnetic field distribution inside the entire area of 500/220 kV substation with double bus bar configuration while the second ingoing power line is switched off.

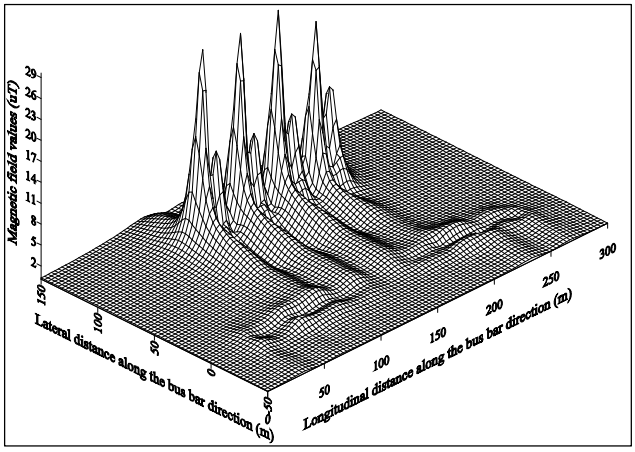

Fig. 9. Magnetic field distribution over the entire area of the simulated 220/66 kV substations with double bus bar configuration (Scenario C).

B. 220/66 kV Substation

Figure 9 presents the magnetic field distribution over the entire area of the 220/66 kV substation with double bus bar horizontal configuration (Scenario C) while all outgoing 66 kV power lines are loaded with 25 MW. The maximum magnetic field value is about 31.5 μT and it is obtained within the area of lower voltage bus bar. Figure 10 presents the magnetic field distribution inside the entire area of 220/66 kV substation for the vertical configuration (Scenario D) while all outgoing 66 kV power lines are loaded with 25 MW. The maximum magnetic field value is about 28.4 μT and it is reduced by about 9.8 % from the corresponding horizontal bus bar configuration.

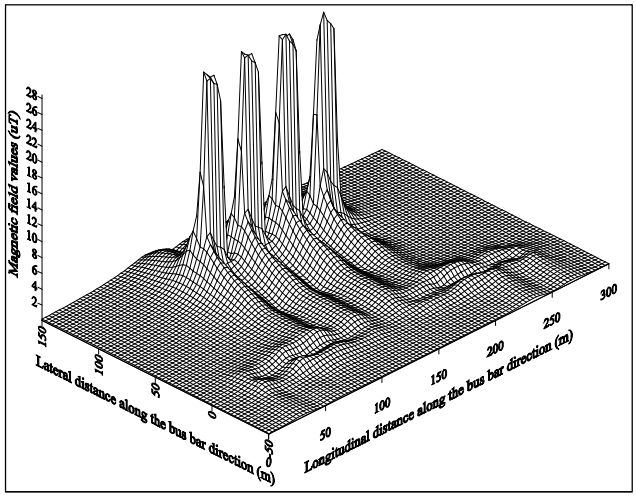

Fig. 10. Magnetic field distribution over the entire area of the simulated 220/66 kV substations with double bus bar (Scenario D).

Figure 11 presents the magnetic field distribution over the entire area of the 220/66 kV substation with double bus bar all vertical configuration (Scenario E) while all outgoing 66 kV power lines are loaded with 25 MW. The maximum magnetic field value is about 7.7 μT and it is obtained within the area of lower voltage bus bar. The maximum magnetic field value is reduced by about 75.5 % from the corresponding horizontal bus bar configuration. Table 1 presents the statistical analysis for the different scenarios regarding considered bus bars arrangements.

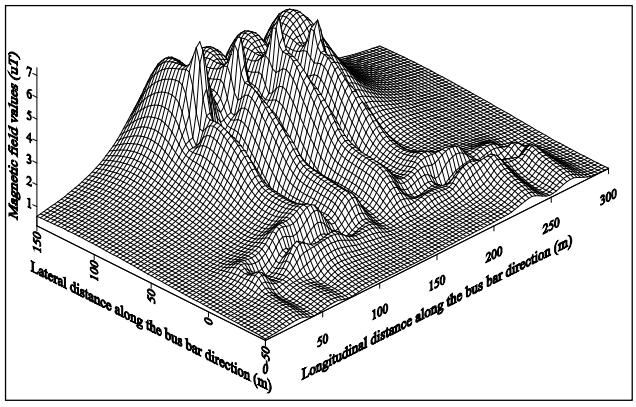

Fig. 11. Magnetic field distribution over the entire area of the simulated 220/66 kV substations with double bus bar for all vertical configuration (Scenario E).

TABLE I. MAGNETIC FIELD STATISTICAL VALUES FOR DIFFERENT BUS BAR CONFIGURATIONS AND ARRANGEMENTS

Bus bar configuration (scenario)	Magnetic field values (μT)			
	Avg	Min	Max	Stdv.
Single 500/220 kV bus bar	0.992	0.038	8.2904	0.939
Single 500/220 kV bus bar, one input offline	1.001	0.038	8.2905	0.949
Double 500/220 kV bus bar	1.314	0.069	13.238	1.347
Double 500/220 kV bus bar, one input off line	1.362	0.074	13.216	1.348
Double 220/66 kV bus bar	1.390	0.102	31.578	2.210
Double 220kV and 66 kV vertical bus bar	1.350	0.081	28.445	2.947
Double bus 220kV and 66 kV all vertical bus bar	1.585	0.128	7.7115	1.397

V. MAGNETIC FIELD MEASUREMENTS

For the validation of the simulation results, the magnetic field measurements are performed 1 m above the ground surface underneath the lower voltage bus bars inside the two simulated high voltage substations and around the transformers. The measurements are performed with actual loading condition for both 500/220 kV substation allocated in West Cairo while the 220/66 kV substation is allocated in the 10th of Ramadan City in East of Cairo. Figure 12 presents the calculated and measured magnetic field value longitudinal profiles under the lower voltage bus bar of 500/220 kV substations. The maximum deviation between the calculated and the measured values is about 9%, which is due to the effects of the metallic structure around the bus bars. Figure 13 presents the calculated and measured magnetic field value longitudinal profiles under the lower voltage bus bar of 220/66 kV substations. The maximum deviation between the calculated and the measured values is about 6% which is due to the effects of metallic structure around the bus bars.

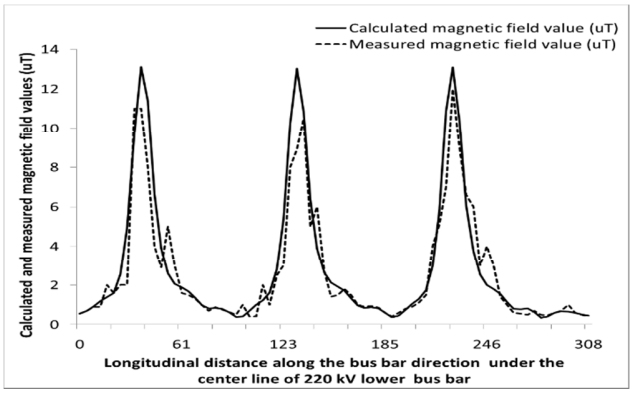

Fig. 12. Calculated and measured longitudinal magnetic field profiles under the center line of the lower voltage bus bar inside the 500/220 kV substation with actual loading conditions.

Figure 14 presents the calculated and measured longitudinal magnetic field values 1 m away from the transformers under the central phase from the lower voltage bus bar side direction inside the 220/66 kV substation with actual loading conditions. The measured magnetic values are higher than the calculated values due to the presence of the transformer windings. The maximum deviation between the maximum measured and calculated magnetic values is about 25%. Figure 15 presents the calculated and measured longitudinal magnetic field values 1 m away from the transformers under the central phase from the higher voltage bus bar side direction inside the 500/220 kV substation with actual loading conditions. Again, the measured magnetic values are higher than the calculated values due to the presence of the transformer windings. The maximum deviation between the maximum measured and calculated magnetic values is about 16%.

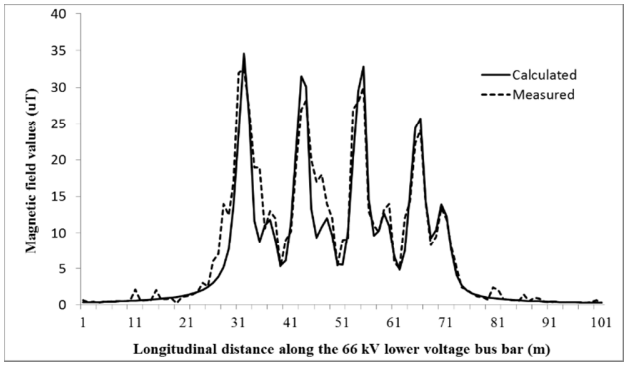

Fig. 13. Calculated and measured longitudinal magnetic field profile under the center line of the lower voltage bus bar inside the 220/66 kV substation with actual loading conditions.

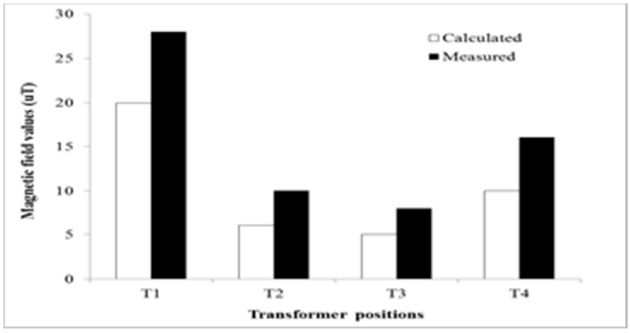

Fig. 14. Calculated and measured longitudinal magnetic field values 1 m away from the transformers under the central phase from the lower voltage bus bar side direction inside the 220/66 kV substation with actual loading conditions.

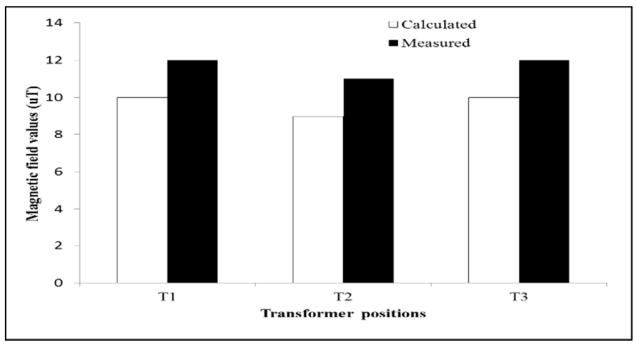

Fig. 15. Calculated and measured longitudinal magnetic field values 1 m away from the transformers under the central phase from the lower voltage bus bar side direction inside the 500/220 kV substation with actual loading conditions.

VI. CONCLUSIONS

Two actual high voltage substations, 500/220 kV and 220/66 kV, are simulated with the MATLAB - M Script developer based on the Biot - Savart law in its general form with the three – dimensions technique. The simulated results are compared with the actual field measurements at different positions inside the simulated substations. Good agreement was noticed between the measured and the calculated magnetic field values under the bus bar area. Meanwhile, the differences between the calculated and the measured values show higher deviation around the transformer due to the higher current inside the transformer windings. For the 500/220 kV substation, the maximum deviation between the measured and calculated magnetic field values is 9% in the area under the bus bars while it reaches 16 % around the transformers. For 220/66 kV substation, the maximum deviation between the measured and the calculated magnetic field values is 6% in the area under the bus bars while it reaches 25 % around the transformers.

REFERENCES

[1] P. Batron, J. Cahouet, and B. Hutzler, "Three-dimensional computation ofthe electric fields induced in a human body by magnetic fields," in *Proceedings of the Eighth International Symposium on High Volt-age Engineering, ISH-1993*, Yokohama, Japan, 1993, Art. no. 9002.

[2] P. S. Maruvada, "Characterization of power frequency magnetic fields in different environments," *IEEE Transactions on Power Delivery*, vol. 8, no. 2, pp. 598–606, Apr. 1993, https://doi.org/10.1109/61.216866.

[3] C. Munteanu, G. Visan, I. T. Pop, V. Topa, E. Merdan, and A. Racasan, "Electric and Magnetic Field Distribution inside High and Very High Voltage Substations," in *2009 20th International Zurich Symposium on Electromagnetic Compatibility*, Zurich, Switzerland, Jan. 2009, pp. 277–280, https://doi.org/10.1109/EMCZUR.2009.4783444.

[4] T. P. Minh *et al.*, "Finite Element Modeling of Shunt Reactors Used in High Voltage Power Systems," *Engineering, Technology & Applied Science Research*, vol. 11, no. 4, pp. 7411–7416, Aug. 2021, https://doi.org/10.48084/etasr.4271.

[5] A. S. Farag, A. Al-Shehri, J. Bakhashwain, and T. C. Cheng, "Electromagnetic Fields in Substations - Sources Modeling and Measurements," presented at the GCC/CIGRE 1995 Meeting, Bahrain, Oct. 1995.

[6] A. S. Safigianni and C. G. Tsompanidou, "Measurements of electric and magnetic fields due to the operation of indoor power distribution substations," *IEEE Transactions on Power Delivery*, vol. 20, no. 3, pp. 1800–1805, Jul. 2005, https://doi.org/10.1109/TPWRD.2005.848659.

[7] C. Munteanu, G. Visan, and I. T. Pop, "Electric and Magnetic Field Distribution Inside High Voltage Power Substations. Numerical Modeling and Experimental Measurements," *IEEJ Transactions on Electrical and Electronic Engineering*, vol. 5, no. 1, pp. 40–45, 2010, https://doi.org/10.1002/tee.20491.

[8] A. P. Anagha and K. Sunitha, "Influence of Field Spacer Geometry on the Performance of a High Voltage Coaxial Type Transmission Line with Solid Dielectric Spacer in Vacuum," *Engineering, Technology & Applied Science Research*, vol. 7, no. 3, pp. 1605–1610, Jun. 2017, https://doi.org/10.48084/etasr.1188.

[9] H. B. Duc, T. P. Minh, T. P. Anh, and V. D. Quoc, "A Novel Approach for the Modeling of Electromagnetic Forces in Air-Gap Shunt Reactors," *Engineering, Technology & Applied Science Research*, vol. 12, no. 1, pp. 8223–8227, Feb. 2022, https://doi.org/10.48084/etasr.4692.

[10] P. Sarma Maruvada, A. Turgeon, and D. L. Goulet, "Study of population exposure to magnetic fields due to secondary utilization of transmission line corridors," *IEEE Transactions on Power Delivery*, vol. 10, no. 3, pp. 1541–1548, Jul. 1995, https://doi.org/10.1109/61.400939.

[11] C. Malagoli *et al.*, "Residential exposure to magnetic fields from high-voltage power lines and risk of childhood leukemia," *Environmental Research*, vol. 232, Sep. 2023, Art. no. 116320, https://doi.org/10.1016/j.envres.2023.116320.

[12] I. Said, A. S. Farag, H. Hussain, and N. A. Rahman, "Measurement of Magnetic Field from Distribution Substations in Malaysia," in *Australasian Universities Power Engineering Conference (AUPEC 2004)*, Brisbane, Australia, Sep. 2004.

[13] I. O. Habiballah, M. M. Dawoud, K. Al-Balawi, and A. S. Farag, "Magnetic Field Measurement & Simulation of A 230 kV Substation," *Proceedings of the International Conference on Non-Ionizing Radiation at UNITEN (ICNIR 2003), Electromagnetic Fields and Our Health*, Oct. 2003.

[14] *Model HI-3604 Survey Meter User Manual*. ETS-Lindgren, Inc., 1992.

[15] *HI-4413 Fiber Optic RS-232 Interface With ProbeView™ 3600 User Manual.* ETS-Lindgren, Inc., 2007.

[16] H. Anis, M. A. Abd-Allah, and S. A. Mahmoud, "Computation of Power Line Magnetic Fields - A Three Dimensional Approach," in *Proceedings 9th International Symposium on High Voltage Engineering (ISH-95)*, Gratz, Austria, 1995, Art. no. 8333.